

The Joint Coordination in Reach-to-grasp Movements

Zhi Li, Kierstin Gray, Jay Ryan Roldan, Dejan Milutinović and Jacob Rosen

Abstract—Reach-to-grasp movements are widely observed in activities of daily living, particularly in tool manipulations. In order to reduce the complexity in redundancy resolution and facilitate upper-limb exoskeleton control in reach-to-grasp tasks, we studied joint coordination in the human arm during such movements. Experimental data were collected on reach-to-grasp movements in a 3-dimensional (3D) workspace for cylinder targets of different positions and grasping orientations. For comparison, reaching movements toward the same targets are also recorded. In the kinematic analysis, the redundant degree of freedom in human arm is represented by the swivel angle. The four grasping-relevant degrees of freedom (GR-DOFs), including the swivel angle and the three wrist joints, behave differently in reach-to-grasp movements comparing to how they behave in reaching movements. The ratio of active motion range (R-AMR) is proposed for quantitatively comparison the task-relevance of the GR-DOFs. Analysis on the R-AMR values shows that the task-relevant GR-DOFs are more actively used, while the task-irrelevant joints are left uncontrolled and maintain their neutral positions. Among the task-relevant GR-DOFs, the smaller joints (micro-structure) are more actively used than the larger joints (macro-structure). The coordination of the task-relevant GR-DOFs is shown to be synergistic. Analysis of the acceleration/deceleration at the GR-DOFs indicates different levels of voluntary control in three phases of the movements. The study of the characteristics of the joint coordination in reach-to-grasp movements provides guidelines for simplifying the control of the upper limb exoskeleton.

I. INTRODUCTION

Reach-to-grasp movements are widely observed in activities of daily living, particularly in tool manipulations. It is critical to study joint coordination of a human arm in reach-to-grasp movements in order to reduce the complexity in redundancy resolution and facilitate control of the upper limb exoskeleton used to support such movements. Although efficient redundancy resolution methods have been proposed to determine the configurations of robotic manipulators [1], [2], yet these general methods are not capable of rendering the natural joint coordination in the human arm. Studies on reaching movements have resolved the kinematic redundancy in the human arm by performance optimizations [3]–[12]. However, arm postures in reach-to-grasp movements are affected by the orientation of the grasp target, and these postures cannot be explained by the motor control strategies that have successfully addressed arm postures in reaching movements [13], [14].

Previous research has investigated the joint coordination in reach-to-grasp movements. Research has shown that hand-

arm coordination is subject to both temporal [15] and spatial constraints [16]. While approaching a target, arm movement directs the thumb, preparing to match the hand orientation with the target [17], [18]. The rotation of the arm plane about the shoulder-wrist axis is coordinated with the supination of the forearm to achieve the desired hand orientation. If the target orientation is perturbed when the hand is moving to the target, the hand orientation begins to match the original target orientation and then adjusts to match the final target orientation [19]. This smooth adaptation to the perturbed target orientation implies that the reach-to-grasp movements may be a superposition of separate reaching and grasping components. Given arm postures predicted for reaching movements, arm postures for reach-to-grasp movements can be constructed based on grasping-related differences. Furthermore, human motor system prefers a joint coordination that minimizes the intervention when redundancy in control variables exists [20], [21]. The control emphasis is placed on task-relevant variables, while task-irrelevant variables are loosely monitored for tolerable variability [22], [23].

This study investigates the spatial and temporal characteristics of the joint coordination in reach-to-grasp movements. Experimental data are collected on the reach-to-grasp movements in a 3-dimensional (3D) workspace, for cylinder targets of different positions and grasping orientations, in addition to the reaching movements toward the targets of the same positions. By kinematic analysis, the grasping-relevant degrees of freedom (GR-DOFs) in the human arm are distinguished from the grasping-irrelevant degrees of freedom (GI-DOFs). Since the kinematic redundancy for reaching movements has been resolved, this paper focuses on the difference between reach-to-grasp and reaching movements and their coordinated spatial and temporal responses to the changes in target position and orientation.

II. EXPERIMENTS

Experimental data were collected to compare the reach-to-grasp movements with reaching movements. During the experiments, nine healthy subjects (three males and six females) conducted specified movements with their right arms. Each subject conducted four sessions of reach-to-grasp movements and one session of reaching movements. Each session consisted of five repetitions of eight different movements. In total, each subject completed $5 \times 8 \times 5 = 200$ trials. During the experiment, the subject sat in a chair with a straight back support. The chair was placed such that the subject could comfortably point at the targets with his/her elbow naturally flexed. The workspace was adjustable so that the center of the workspace was aligned with the right

Zhi Li (zhil@soe.ucsc.edu), Kierstin Gray (kngay@ucsc.edu), Jay Ryan Roldan (juroldan@ucsc.edu), Dejan Milutinović (dejan@soe.ucsc.edu) and Jacob Rosen (rosen@soe.ucsc.edu) are with the Department of Computer Engineering, University of California, Santa Cruz, CA 95064, USA

Bionics Lab URL: <http://bionics.soe.ucsc.edu/>

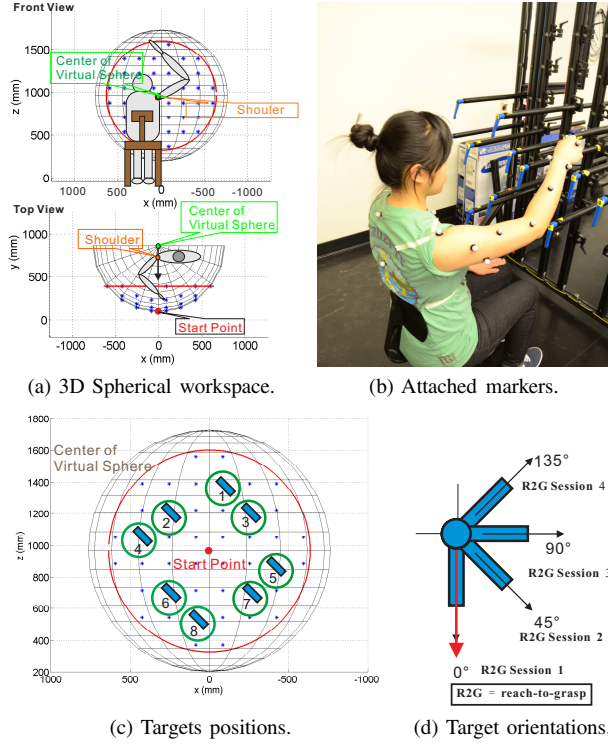


Fig. 1: (a) The right shoulder of the subject is aligned with the center of the spherical workspace. (b) Markers are attached to the right arm and the torso for position tracking. (c) Eight targets are involved in the reach-to-grasp experiment. (d) In the four reach-to-grasp sessions, the handles are oriented at 0° , 45° , 90° , 135° on the plane that the subject face to, with respect to the direction of gravity.

shoulder. In this configuration, the right arm is free to move, while the torso is set against the chair back to minimize the shoulder movements. The target arrangement is shown in Fig. 1c. In the reaching session, at a “start” command, the subjects pointed from the start point (shown in Fig. 1a and Fig. 1c) to the instructed target with their index finger in line with the forearm. In the reach-to-grasp sessions, the subject started with pointing to the start point and reached to grasp the instructed handles with firm power grasp. As shown in Fig. 1b, passive reflective markers are attached to the torso and the right arm of the subjects. A motion capture system records the movement at the frequency of 100 Hz. To avoid fatigue, subjects rested after each session.

III. METHODOLOGY

A. The Grasping-relevant DOFs in the Human Arm

In reach-to-grasp movements, the arm postures are significantly affected by the grasping position and orientation. To distinguish the grasping-relevant degrees of freedom from the grasping-irrelevant degrees of freedom, this section performs motion analysis based on a kinematic model of the human arm. As shown in Fig. 2a, the seven kinematic joints in human arm are: shoulder abduction θ_1 , shoulder flexion θ_2 , shoulder rotation θ_3 , elbow flexion θ_4 , supination θ_5 , wrist flexion θ_6 and radial deviation θ_7 . Due to the kinematic

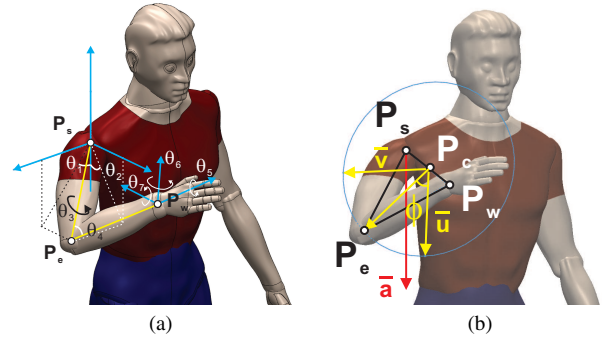


Fig. 2: (a) The kinematic modeling of human arm has seven DOFs. (b) The rotation of the arm plane about the shoulder-wrist axis is measured by the swivel angle ϕ .

redundancy, when the wrist position and grasping orientation are specified, the elbow can still move around the axis going through the shoulder and wrist position. In the kinematic modeling, we use the wrist position P_w and the swivel angle ϕ instead of Joint Angle 1 to 4. Therefore, kinematic redundancy is fully accounted by only one variable. As shown in Fig. 2b, the direction of elbow pivot axis (denoted by \vec{n}) is defined as:

$$\vec{n} = \frac{P_w - P_s}{\|P_w - P_s\|} \quad (1)$$

A plane orthogonal to \vec{n} can be determined given the position of P_e . Point of intersection between the orthogonal plane and the vector $\overrightarrow{P_w - P_s}$ is P_c . $\overrightarrow{P_e - P_c}$ is the projection of the upper arm $(P_e - P_s)$ on the orthogonal plane. \vec{u} is the projection of a normalized reference vector \vec{a} onto the orthogonal plane, which can be calculated as:

$$\vec{u} = \frac{\vec{a} - (\vec{a} \cdot \vec{n})\vec{n}}{\|\vec{a} - (\vec{a} \cdot \vec{n})\vec{n}\|} \quad (2)$$

The swivel angle ϕ , representing the arm posture, is defined by the angle between the vector $\overrightarrow{P_e - P_c}$ and \vec{u} . If the reference vector \vec{a} is $[0, 0, -1]^T$, then the swivel angle $\phi = 0^\circ$ when the elbow is at its lowest possible point [24]. The motion range at the elbow is limited in order to avoid the singularity at extreme elbow flexion and extension.

By representing the kinematic redundancy with the swivel angle, the grasping-relevant DOFs are distinguished from the grasping-irrelevant DOFs: the three DOFs for wrist positions remain the same for both reaching and reach-to-grasp movements, while the swivel angle and the three wrist joints will be affected by grasping position and orientation. Since the kinematic redundancy has been resolved for reaching movements [], the following analysis will focus on the four grasping-relevant DOFs (GR-DOFs) and investigate their spatial and temporal responses for different target positions and orientations.

B. Data Normalization and Component Separation

During the experiments, the trajectories of the markers are recorded and the trajectories of the four GR-DOFs are computed by inverse kinematics. These trajectories were normalized relative to the percentage of the path length traversed by the hand (instead of time) and averaged based on five repetitions of the same movement. With reference to the reaching movements, grasping-related differences are computed so that the reaching component can be separated from the grasping component. This component separation is applied to the four GR-DOFs, including the swivel angle and the three wrist DOFs.

C. The Ratio of Active Motion Range

In joint coordination, the joints that are actively used respond more to the changes in task specifications than the joints not actively involved in the movements. The **ratio of the active motion range (R-AMR)** for each GR-DOF is computed to evaluate the responses of the grasping component of the GR-DOFs to the changes in target position and orientation. At the end of the movements, we computed the standard deviation of the value of the grasping component for each GR-DOF across different movements. The R-AMR is then defined as the ratio between this standard deviation and half of the motion range of this GR-DOF. Note that the R-AMR can be computed across different movement sets, including movements to targets at a particular position or in a particular orientation. For a movement set, a large R-AMR value indicates that that particular DOF is sensitive to the task parameters that vary within that movement set. For example, the R-AMR of a DOF across reach-to-grasp movements towards a particular target position with different orientations indicates the sensitivity of that DOF to target orientation. Likewise, the R-AMR of a DOF across movements to different targets that share the same orientation indicates sensitivity to target position.

IV. RESULTS

A. The Reaching and Grasping Components.

This section presents results from the analysis of the grasping components of the reach-to-grasp movements. Prior to computing the R-AMR values for each GR-DOF, the data collected on reach-to-grasp movements were processed by data normalization and component separation. Fig. 3 shows an example of data normalization of the swivel angle in the trials collected from a representative subject. In Fig. 3a, swivel angle trajectories regarding to the same individual target are normalized with respect to hand path length. The averaged trajectory of five repetitions of each movement is shown in Fig. 3b. With reference to the reaching movement, each reach-to-grasp movement to the same target is separated into a reaching component (Fig. 3c) and a grasping component (Fig. 3d). A grasping component is computed as the difference between the reaching movement and the reach-to-grasp movement to the same target but of different grasping orientation.

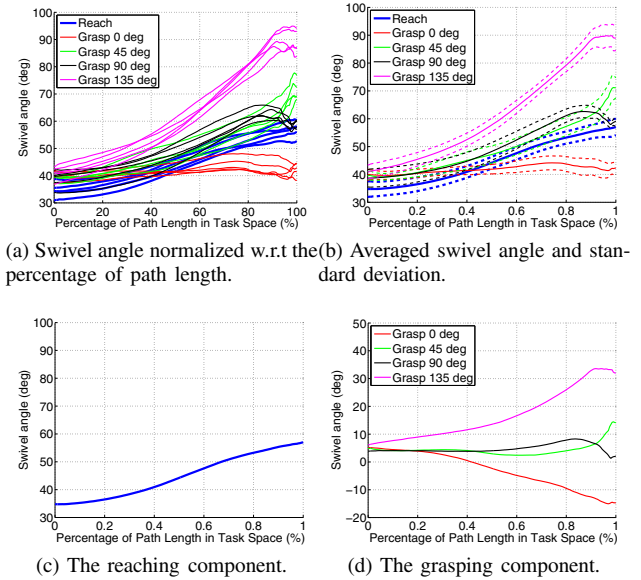


Fig. 3: (a) The swivel angle trajectories are normalized with respect to the percentage of path length. (b) The averaged trajectories are found with their time-varying standard deviation. With reference to the averaged trajectory of the reaching movement, the reach-to-grasp movements can be separated into (c) the reaching component and (d) the grasping component.

In Fig. 4, component separation is applied to the data from a representative subject for each GR-DOF. The reaching components of all the GR-DOFs are approximately linear with respect to the percentage of the hand path length. The reaching components of the swivel angle vary for different targets, while the reaching components of the other GR-DOFs are mostly constant. In reaching movements, the index finger is aligned with the forearm, which results in little movement of forearm pronation-supination. With regard to the grasping components, the swivel angle and the forearm pronation-supination is linear for most of the path length percentages. The flexion-extension and radial deviation at the wrist are nonlinear. The nonlinear flexion-extension during the movement is possibly due to opening and closing of the hand aperture preparing for grasping.

Fig. 5 shows the second derivative of the grasping components of the four GR-DOFs. During the reach-to-grasp movements, each GR-DOF experiences three distinguishable phases with different amounts of acceleration/deceleration. The first 10% – 20% of the movement is the “pre-match” phase. Knowing the designated target orientation, subjects coordinate the four grasping variables for matching the hand orientation with the target orientation. After the pre-match phase, there is a period during which there is no significant change in the acceleration of the variables. After 60% – 80% of the path length, the hand has been transported close enough to the target such that the four variables are adjusted for closing the hand and for matching the hand with the target more precisely. The second phase is called the “transportation phase” and the third phase is called the “match phase”. Regarding the temporal responses of the GR-DOFs, the three

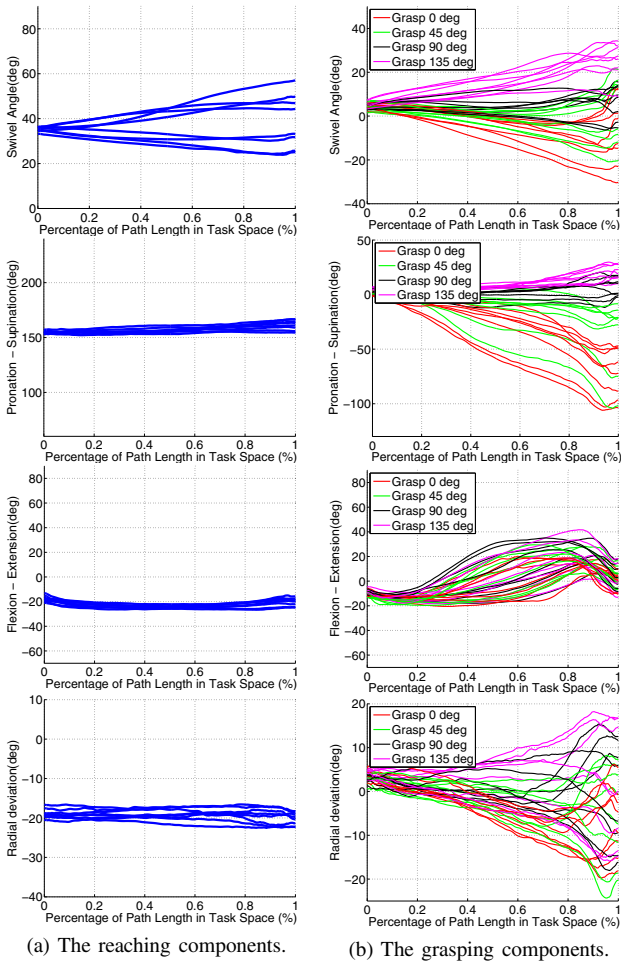


Fig. 4: The reaching and grasping components of the swivel angle (ϕ), pronation-supination (θ_5), flexion-extension (θ_6) and radial deviation (θ_7).

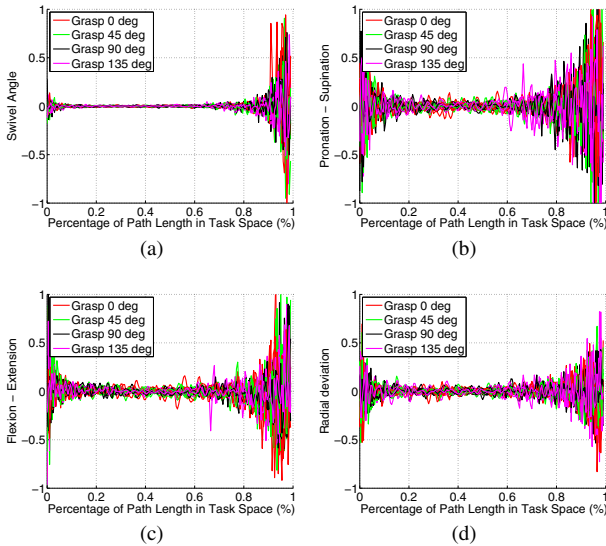


Fig. 5: Second order derivative of the grasping component.

distinguishable amounts of acceleration/deceleration indicate

different levels of voluntary control in different phases of motion.

B. The Active Motion Range of Different Grasping Variables

This section presents the R-AMR values of the grasping components for each GR-DOF at the end of the movements. For each subject, the R-AMR values are computed across all target positions and orientations. Fig. 6 summarizes the R-AMR values of all the subjects for each GR-DOF. Among the four GR-DOFs, the pronation-supination and radical deviation are more actively used than the other two GR-DOFs. Note that for the experimental setup, both the swivel angle and the pronation-supination can be used for adjusting the hand orientation according to the target. In Fig. 6, the pronation-supination is more actively used than the swivel angle. The flexion-extension is least sensitive to the changes in target position and orientation due to its low task-relevance, which confirms the limited usage of flexion-extension described by [25].

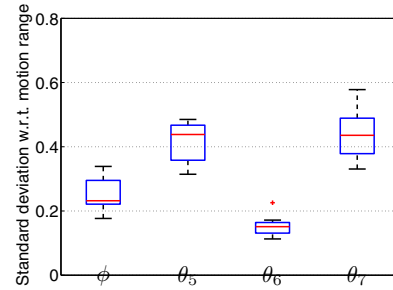


Fig. 6: The R-AMR values are computed for each subject across all the target position and orientations. The higher R-AMR values indicate more active usage of the GR-DOF.

C. The Coordination of Task-relevant GR-DOFs

Section IV-B has shown that the GR-DOFs of higher task-relevance are more actively used, which inspires a study of their coordination. During the experiment, the target orientation only changes in the plane that the subject faces. As a result, hand orientation is cooperatively adjusted by the swivel angle and pronation-supination. When the target orientation is greater than 90° , the swivel angle is largely used to provide comfortable grasping postures. To investigate this task-dependent coordination of the GR-DOFs, for each subject, we computed the average of the end values of the grasping components of a GR-DOF across all target positions for the same target orientation. The average end values corresponding to different target orientations form the response of a GR-DOF to the change in target orientation. In Figures 7a and 7b, each solid blue line represents the response of a subject to target orientations. The associated dashed blue lines are the third-order spline regressions. The averaged response of all subject is represented by a solid red line, bounded by two red dash lines that represent the standard deviation. While Figures 7a and 7b describe the responses at the swivel angle and the pronation-supination, Fig. 7c shows the changes of hand orientation resulting from their

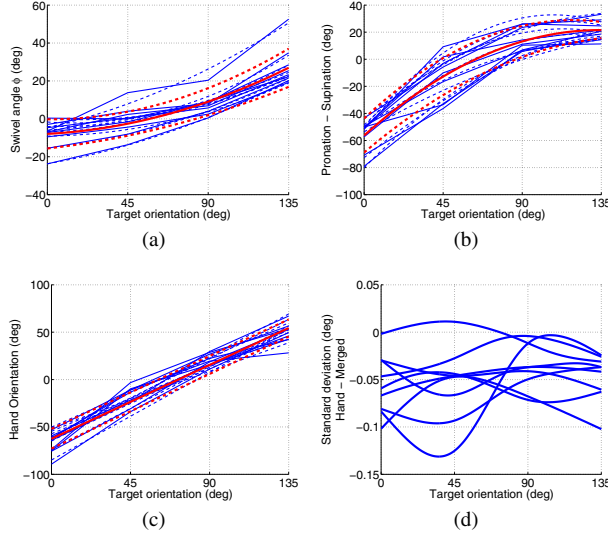


Fig. 7: The averaged response of grasping component for (a) the swivel angle, (b) the pronation-supination and (c) the hand orientation. (d) $\sigma_\eta - (\sigma_\phi^2 + \sigma_{\theta_5}^2)^{1/2}$ is negative, indicating that the swivel angle and the pronation-supination exhibit synergy.

task-dependent coordination. Denoting the target orientation by φ and the hand orientation by η , the coordination of the nonlinear responses of the swivel angle and pronation-supination results in an approximately linear response in hand orientation (see Equations (3) and (4)).

$$\phi = 0.0015\varphi^2 + 0.0502\varphi - 7.9475 \quad (3)$$

$$\theta_5 = -0.0043\varphi^2 + 1.1630\varphi - 56.3191 \quad (4)$$

$$\eta = 0.8658\varphi - 62.4985 \quad (5)$$

For each subject, we computed the standard deviations across the target position for the end values of the swivel angle, the pronation-supination and the hand orientation, denoted by σ_ϕ , σ_{θ_5} and σ_η , respectively. The standard deviations are computed based on the regression of variable responses and cover the target orientation range from 0 to 135°. To analyze the variance of the coordinated joints and their resulted hand orientation, we compute $(\sigma_\phi^2 + \sigma_{\theta_5}^2)^{1/2}$ and compare it to σ_η . Fig. 7d shows $\sigma_\eta - (\sigma_\phi^2 + \sigma_{\theta_5}^2)^{1/2}$ values are mostly negative for all the nine subjects, which indicates that the coordination of swivel angle and the pronation-supination is synergetic [26].

V. DISCUSSION

In reach-to-grasp movements, arm posture is significantly affected by grasp orientation. The kinematic analysis on human arm has indicated that compared to joint coordination in reaching movements, human arm only behaves differently at the four grasping-relevant degrees of freedom (GR-DOFs), including the swivel angle, the pronation-supination, the wrist flexion and the radial deviation. As a result, this research focused on the four GR-DOFs and separated their grasping components from their reaching components.

A. The Task-dependent Coordination of GR-DOFs

Investigations of the grasping components of the GR-DOFs have indicated that the coordination of the GR-DOFs are task-dependent. Comparing their ratios of active motion range (R-AMR), the task-relevant GR-DOFs are more actively used, while the task-irrelevant joints are left uncontrolled. In the reach-to-grasp experiments, the target orientation varies in the plane that the subject faces, which demands the cooperative responses of the swivel angle and the pronation-supination. The wrist flexion is least useful for matching hand orientation to target orientation and therefore its joint angle does not vary much for different target positions and orientations. To minimize the control effort, such task-irrelevant joints are preferably maintained at their neutral positions [21].

The analysis on the R-AMR values further pointed out that among the task-relevant GR-DOFs, the smaller joints are more actively used than the larger joints. In the control of robotic manipulator, the macro and micro joints has been assigned with different control priorities in the trajectory tracking task. In [27], a flexible macro-structure that moves quickly over a wide range of motion is mainly responsible for the task, while a rigid micro-structure compensates for tracking errors. In the context of reach-to-grasp movements, one way to segment the macro/micro structures refers to the arm as a macro mechanism and the hand as a micro mechanism. As such, the arm as a gross positioner is manipulable to maximize the dexterity of the hand as the micro manipulator which is responsible for accomplishing the task [28], [29]. To adjust the hand orientation, since the swivel angle (macro) and the pronation-supination angle of the forearm (micro) can serve the same purpose, it is more energy-efficient to adjust the pronation-supination angle of the forearm as opposed to the swivel angle if the target orientation is within the range of motion of the forearm.

The coordination of the task-relevant GR-DOFs has been analyzed by their responses to the changes in target orientation. As shown in Fig. 7d, the total variance of the swivel angle and the pronation-supination is less than the variance in their resulted hand orientation, which indicates that the coordination of the task-relevant GR-DOFs is in synergy. Studies on the variability of human motion have pointed out that motor synergy reduces the computational complexity of motor control. It is generally applicable to different levels of motor activities (neural, muscular, dynamic, kinematic, etc.), and appropriate for coordinating the numerous degrees of freedom in the body [30]. In previous research, the motor synergy has been found in the two-finger force production task [26]. As an original contribution, this paper provides a method to measure the task-relevance of the GR-DOFs and provides further evidence of the motor synergy of the task-relevant GR-DOFs in multiple joint coordination.

B. On the Control of the Upper Limb Exoskeleton

Studies on the joint coordination in reach-to-grasp movements provide useful guidelines for the control of the upper

limb exoskeleton. The separation of the reaching and grasping components shows that the redundancy resolution of the reach-to-grasp movements can take advantage of existing redundancy resolution methods for reaching movements. During the movements, the grasping components of the swivel angle and pronation-supination are mostly linear with respect to the percentage of the hand path length. In response to the changes in the target orientation, the end values of these two synergistically coordinated GR-DOFs may follow the proposed regression (see Equations (3) to (5)). For reach-to-grasp tasks similar to the experiments described in this paper, the end values of the radial deviation varies more across target position than across target orientation. At the end of the movements, the flexion-extension can be constrained to its neutral position to reduce the control complexity. Regarding the temporal responses of the GR-DOFs, the analysis of acceleration/deceleration shows that the reach-to-grasp movement has three distinguishable phases with different levels of voluntary control. As a result, this research suggests that feed-forward control be used during the first 80% of the path length and feedback control for precisely matching the hand orientation with the target orientation.

REFERENCES

- [1] L. Sciavicco, "A solution algorithm to the inverse kinematic problem for redundant manipulators," *IEEE Trans. Robot. Automat.*, vol. 4, no. 4, pp. 403–410, 1988.
- [2] J. Hollerbach and K. Suh, "Redundancy resolution of manipulators through torque optimization," *IEEE Trans. Robot. Automat.*, vol. 3, no. 4, pp. 308–316, Aug. 1987.
- [3] H. Asada and J. Granito, "Kinematic and static characterization of wrist joints and their optimal design," in *ICRA 1985*, St. Louis, Missouri, Mar. 1985, pp. 244–250.
- [4] T. Yoshikawa, "Dynamic manipulability of robot manipulators," in *ICRA 1985*, St. Louis, Missouri, Mar. 1985, pp. 1033–1038.
- [5] —, *Foundations of Robotics: Analysis and Control*. The MIT Press, 1990.
- [6] H. Kim, L. Miller, and J. Rosen, "Redundancy resolution of a human arm for controlling a seven dof wearable robotic system," in *EMBC 2011*, Boston, USA, Aug. 2011.
- [7] J. Soechting, C. Buneo, U. Herrmann, and M. Flanders, "Moving effortlessly in three dimensions: does donders' law apply to arm movement?" *J. Neuroscience*, vol. 15, no. 9, pp. 6271–6280, 1995.
- [8] T. Kang, J. He, and S. I. H. Tillery, "Determining natural arm configuration along a reaching trajectory," *Exp Brain Res*, vol. 167, pp. 352–361, 2005.
- [9] N. Hogan, "An organizing principle for a class of voluntary movements," *J. of Neuroscience*, vol. 4, no. 2, pp. 2745–2754, 1984.
- [10] T. Flash and N. Hogan, "The coordination of arm movements: an experimentally confirmed mathematical model," *J. of Neurophysiology*, vol. 5, pp. 1688–1703, 1985.
- [11] Y. Uno, M. Kawato, and R. Suzuki, "Formation and control of optimal trajectory in human multijoint arm movement - minimum torque-change model," *Biology Cybernetics*, vol. 61, pp. 89–101, 1989.
- [12] E. Nakano, H. Imamizu, R. Osu, Y. Uno, H. Gomi, T. Yoshioka, and M. Kawato, "Quantitative examinations of internal representations for arm trajectory planning: Minimum commanded torque change model," *The Journal of Neurophysiology*, vol. 81, no. 5, pp. 2140–2155, 1999.
- [13] S. Tillery, T. Ebner, and J. Soechting, "Task dependence of primate arm postures," *Experimental Brain Research*, vol. 104, no. 1, pp. 1–11, 1995.
- [14] J. Soechting and M. Flanders, "Parallel, interdependent channels for location and orientation in sensorimotor transformations for reaching and grasping," *J. of Neurophysiology*, vol. 70, no. 3, pp. 1137–1150, 1993.
- [15] M. Jeannerod, "The timing of natural prehension movements," *J. Neurophysiology*, vol. 16, no. 3, pp. 235–254, 1984.
- [16] M. Mon-Williams and J. Tresilian, "A simple rule of thumb for elegant prehension," *Curr. Biol.*, vol. 11, no. 13, pp. 1058–61, 2001.
- [17] P. Haggard and A. Wing, "On the hand transport component of prehensile movements," *Curr. Biol.*, vol. 29, no. 3, pp. 282–7, 2001.
- [18] J. Smeets and E. Brenner, "A new view on grasping," *Motor Control*, vol. 3, pp. 237–271, 1999.
- [19] J. Fan, J. He, and S. Tillery, "Control of hand orientation and arm movement during reach and grasp," *Exp. Brain Res.*, vol. 171, no. 3, pp. 283–96, 2006.
- [20] E. Todorov and M. I. Jordan, "Optimal feedback control as a theory of motor coordination," *Nature Neuroscience*, vol. 5, pp. 1226–1235, 2002.
- [21] E. Todorov, "Optimality principles in sensorimotor control," *Nature neuroscience*, vol. 7, pp. 907–915, 2004.
- [22] J. P. Scholz and G. Schoner, "The uncontrolled manifold concept: identifying control variables for a functional task," *Experimental brain research*, vol. 126, no. 3, pp. 289–306, 1999.
- [23] M. Latash, *Synergy*. Oxford University Press, USA, 1 edition, 2008.
- [24] N. I. Badler and D. Tolani, "Real-time inverse kinematics of the human arm," *Presence*, vol. 5, no. 4, pp. 393–401, 1996.
- [25] X. Wang, "A behavior-based inverse kinematics algorithm to predict arm prehension posture for computer-aided ergonomic evaluation," *J. Biomechanics*, vol. 32, no. 5, pp. 453–460, 1999.
- [26] M. Latash, "Motor synergies and the equilibrium-point hypothesis," *Motor Control*, vol. 14, no. 3, p. 294C322, 2010.
- [27] Y. Nakamura, H. Hanafusa, and T. Yoshikawa, "Task-priority based redundancy control of robot manipulators," *IJRR*, vol. 6, pp. 3–15, 1987.
- [28] O. Khatib, "Inertial properties in robotic manipulation: An object-level framework," *IJRR*, vol. 5, pp. 19–36, 1995.
- [29] J. Huang, M. Hara, and T. Yabuta, "Controlling a finger-arm robot to emulate the motion of the human upper limb by regulating finger manipulability," in *Motion Control*, F. Casolo, Ed. INTECH, 2010, pp. 773–792.
- [30] N. Bernstein, *The coordination and regulation of movements*. Oxford, New York: Pergamon Press, 1967.